Source, Path, and Site Ground Motion Model of The Loma Prieta Earthquake: Preliminary Results

W. J. Silva
Pacific Engineering and Analysis

C. Stark
Graduate Student, U.C. Berkeley

ABSTRACT

The objective of this study is to model the observed strong ground motion variability during the 1989 Loma Prieta earthquake. The modeling exercise is intended to assess the effects of source finiteness, crustal propagation, and site response upon the recorded motions. The ground motion model employed combines a model for the finite earthquake source as well as nonlinear soil response and crustal propagation effects with the band-limited-white-noise (BLWN) ground motion model. The combined model uses random vibration theory (RVT) to produce site specific estimates of peak acceleration and response spectral ordinates. Preliminary results indicate that the simple point-source using a 1/distance geometrical attenuation provides the optimum overall fit to observed response spectra at fault distances ranging from 1 - 80 km. In addition, knowledge of site specific kappa values reduce the uncertainty in spectral estimates for frequencies exceeding 3 - 4 Hz.

INTRODUCTION

In the near-source region of large earthquakes, dynamic and geometrical properties of the extended (or finite) earthquake source may profoundly affect the resulting ground motion. Specific properties such as rupture propagation, directivity, and source-receiver geometry may be incorporated into strong ground-motion predictions. In this study, a model for the finite-source is combined with the BLWN-RVT ground-motion model [1] to produce site-specific response spectra appropriate for engineering design. The site-response calculation includes nonlinear effects of strain-dependent soil properties on vertically propagating shear waves. In addition, to accommodate the effects of crustal structure on wave propagation at large distances ($\geq$ 50 km), the model incorporates the contributions of direct and supercritically reflected wavefields [2]. Together with the finite-source model, this combined approach yields a site-response methodology applicable to a wide range of site conditions and source distances. As a result, the model is useful in isolating and quantifying the source, propagation path, and site properties which control the variability of strong ground motions. This assessment is made by modeling a total of 25 strong motion sites (22 rock and 3 soil) which recorded the 1989 Loma Prieta earthquake. For these sites, fault distances ranged from 1 to 81 km (Table 1).

COMPUTATIONAL MODEL

To approximate the effects of an extended source at close source-receiver distances, the empirical Green function methodology [3] is followed, but in place of small-earthquake recordings the omega-square source model [4], is used to simulate a series of small earthquakes distributed across the fault plane. The model assumes constant slip in small, discretized sub-faults, and generates a small-magnitude source function over each area. The initiation of slip on the sub-fault is partially randomized to minimize artificial periodicity of sub-events. By propagating the rupture across a series of sub-faults, appropriately time-delayed, the model generates a Fourier spectrum which incorporates the effects of rupture propagation. This spectrum is then used to estimate response spectra for a finite- source within the framework of the BLWN-RVT ground-motion model. Path effects are approximated with factors for geometrical spreading (1/distance) and frequency-dependent attenuation. Amplification factors for rock sites are modeled by vertical propagation of motions through a crustal velocity model, with the near-surface exponential-decay parameter kappa [5]. At soil sites, motions are additionally propagated

through a soil profile, using an equivalent-linear approach to model the effects of strain-dependent shear modulus and damping values [6]. In order to model the effects of direct and supercritically-reflected S- waves, the point-source part of the model has been augmented to include the contributions of these wavefields [2]. This extension of the BLWN model then permits an evaluation of the appropriateness of the simple assumption of 1/distance [1] for geometrical attenuation.

INITIAL MODEL RESULTS

The M 6.9 1989 Loma Prieta earthquake produced a wealth of strong-motion recordings at source-receiver distances of less than 100 km, representing a variety of site conditions. The source model employed here is given by the slip distribution of Wald et al. [7]. The slip distribution is approximated using a grid of 3.3-by-2.5 km patches of constant slip, with each sub-event having M 5.0. Slip is initiated across the fault using a constant rupture velocity (circular rupture front) of 3 km/sec. The total rupture duration is 6.5 sec and the rise time is 1.2 sec.

In the first step of the project, rock outcrop motions at 22 rock sites at fault distances from 1 to 81 km (Table 1) were modeled. Using templates for spectral shapes as a function of kappa for an M 6.9 point-source at close distances [8], kappa values were determined for each rock site (Table 1, model 0); the average kappa is .06 sec. For crustal amplification, the velocity model of Wald et al. [7] was used. The Q model used is appropriate for WNA; $Q(f) = 150\ f^{0.6}$ (Table 1, model 0 [8]). Acceleration response spectra (5% damped) in the band .010 to 10 sec, were then simulated for the finite-fault model and for an equivalent point-source model, both using the simple 1/R geometrical term. For the point-source simulations, the magnitude and source durations were constrained to M 6.9 and 6.0 sec respectively [7]. These values result in a Brune stress drop of 238 bars for a source region shear-wave velocity of 3.6 km/sec at a depth of 12 km (depth of the largest asperity [7]). Comparisons of these simulations to the average of two horizontal components recorded at 9 of the 22 rock sites are shown in Figure 1.

In addition, response spectra were modeled at three soil sites: PAV (stiff soil), GL2 (deep stiff soil), and TRI (soft soil)(Table 1). Shear-wave velocity profiles for these sites (from surface to bedrock) are derived from downhole seismic surveys performed in close proximity to each of the strong-motion instruments (Bruce Redpath, personal communication). Shear modulus and damping for PAV and TRI sites as functions of shear strain used in the modeling are shown in Figure 2. The soil models are preliminary and currently are based upon strong-motion simulations. The soil models for GL2, also shown in Figure 2, are preliminary results from laboratory tests (Ken Stokoe, personal communication). Further refinement of the models will result from an ongoing laboratory-testing program. For input to the soil column, the same crustal velocity model was used, with a kappa of .04 sec appropriate for average western North America rock sites [8]. The soil columns were then simply placed on top of the crustal model. Comparisons of simulations to observations at soil sites are shown in Figure 1.

For rock sites, both the finite-fault and point-source models generally simulate the observed peak acceleration and spectral shape over broad spectral ranges. For periods shorter than 1.0 sec, the finite and point-source models appear to fit the data equally well. At close distances, within 20-30 km, the point-source clearly overpredicts long-period ($>$ 1.0 sec) response. At all distances, the finite-source model generally appears deficient at intermediate periods (0.5 - 3.0 sec). We attribute this deficiency to the manner in which small-magnitude earthquakes are summed to generate large earthquakes in the simulation [10].

For the soil sites (GL2, PAV, and TRI), the simulated motions agree very well for periods less than about 0.3 sec. As with the rock sites, the finite-source shows some spectral deficiency at intermediate periods and the point-source overpredicts at long periods at the close sites. For the distant soil site, TRI, the fit is very good from peak acceleration to periods of several seconds.

To illustrate the effects of soil nonlinearity at high levels of motion, Figure 3 shows 5% damped response spectra resulting from a site response analysis at GL2 using the outcrop recorded motions at GL1 as control motions. In Figure 3, the dash-dotted line represents a linear analysis using the small strain laboratory data. The resulting motions show exaggerated short period response with a peak acceleration of 0.76 g. The equivalent-linear analysis shows a good fit over the entire bandwidth with a peak acceleration of 0.37 g, in accord with the average observed of 0.37 g. The improvement at long periods using the nearby rock outcrop as control motions over the point-source model is a consequence of the exaggerated long period response of the point-source model at long periods. Also shown in Figure 3 are the low- and high- strain values of shear-wave velocity and Q (damping $\approx$ 1/2Q).

STRONG MOTION DATA INVERSION

In order to provide a more region-and site-specific ground motion model, an inversion for magnitude, corner frequency (inverse of source duration), regional Q model (Q_o and eta), and site specific kappa values was made for the 22 rock sites. Using the starting values from model 0 (Table 1), the resulting model parameters are shown in Table 1 as model 1. Interestingly, the average kappa value is changed little (0.06 sec to 0.05 sec). The moment magnitude has decreased slightly to 6.86 with an increase in duration to 6.2 sec resulting in a Brune stress drop of 184 bars. Of particular interest, the Q model has shown an increase in Q_o to 186 and a decrease in eta to 0.36. Apparently the system is more compatible with a higher Q_o and less of a frequency dependence than that assumed appropriate for WNA.

INVERSION MODEL RESULTS

Both the finite- and point- source models were rerun with the new model parameters (Table 1, model 1). For the finite-source however, the source model, based upon Wald et al. [7], was left unchanged. The simulated peak acceleration values are shown in Table 1. The results of the inversion generally show an increase in motions for the point-source resulting in a slightly better fit at distance. For the finite-source, while the motions are generally comparable, care should be taken in evaluating the difference because a point-source model was used in the inversion and neither the magnitude nor source duration was perturbed in the finite-fault run.

To provide a quantative measure of the ground motion predictions, a simple goodness of fit at each spectral period was performed by taking the difference of the logs of the observed average response spectrum and the predicted response spectrum, squaring, and summing over the 22 rock sites. Dividing the resultant by the number of sites (assuming zero bias) results in an estimate of the model variance. Figure 4 shows the natural log of the standard error plotted versus frequency for the finite- and point- source simulations using model 0 (Table 1) parameters (top frame) and model 1 parameters (lower frame). For both the point- and extended- sources, the standard errors for frequencies greater than about 2-3 Hz are comparable to those based upon empirical regression analyses. The large peak shown in the finite-fault standard error is a consequence of the intermediate-period spectral deficiency of the response spectra shown in Figure 1. Additional features of interest include the small difference between the point and extended source models and the stability of the point- source standard error to periods of several seconds. The increase in the point-source standard error with increasing period is due largely to the overprediction at close distances shown in Figure 1. For model 1, shown in Figure 4 (lower), there is a reduction in standard error for the point-source and a slight increase for the finite-source.

To examine the distance dependency of the difference in standard errors between the point- and finite- sources, Figure 5 shows an analogous set of plots for sites located within a fault distance of 55 km (sites including A2E and closer). For model 0, the finite-source shows a generally lower variance than the point-source for high frequencies ($>$ 4 Hz). Comparable levels of uncertainty are shown down

to about 1 Hz where the finite-fault spectral deficiency peaks. Also, the overprediction of the point-source at long periods is apparent in the increase in standard error at low frequencies. The value at 0.1 Hz exceeds that shown in Figure 4 by a significant amount supporting the observation that the low frequency misfit is due largely to the close stations. This may be a consequence of using an average radiation pattern coefficient in the point-source model as well as in the inversion code.

The model 1 results in Figure 5 show an improved fit for the point-source and an increase in error for the finite-source, particularly at high frequencies. Apparently, for the close-in stations, inversions for source, path, and site properties should include effects of source finiteness. However, it must be recalled that the finite-fault simulations were not rerun with a lower magnitude and slightly larger duration which resulted from the point-source inversion (Table 1, model 1).

Considering the standard errors shown in Figure 4 for all sites (1 - 81 km) and Figure 5 for the close-in sites, it appears there is not a large difference in uncertainty between the point- and extended-sources. The simple point-source, given the proper source and propagation path parameters, as well as site-specific kappa values, produces response spectral ordinates that are, on average, as reliable as those produced with a finite source.

EFFECTS OF KAPPA

In the stochastic model used here the controlling site-dependent parameter for rock sites is kappa [5,8]. In order to assess the overall improvement in fit that site-specific kappa values can provide, the point-source simulations were run with a constant average kappa. The value used (0.05 sec) is the average resulting from the inversion (Table 1, model 1). Figure 6 shows the results for all rock sites compared to the point-source with site-specific kappa values. As expected, the constant kappa variance is larger than the site-specific kappa simulations and the difference is frequency dependent. For frequencies less than about 3 - 4 Hz, site-specific kappa values provide little reduction in variance. For higher frequencies, however, the reduction in uncertainty appears to be significant and demonstrates that knowledge of an appropriate kappa value for a particular site is significant in predicting expected motions.

To examine the goodness of fit of the point-source model using a 1/R geometrical attenuation to the observed attenuation of peak acceleration, Figure 7 shows the model 1 predictions along with a curve computed using the model 1 average kappa of 0.05 sec. The model with site specific kappa values provides an acceptably good fit (standard error of about .034) to the data. The constant kappa model has a standard error for peak acceleration of about 0.47, which is still comparable to that obtained from empirical regression analyses which include interearthquake variability. The two extreme outliers in the data at about 80 km with average peak horizontal accelerations near 0.2 g are sites Presidio and Golden Gate. It is possible that these sites, which are located upon soft serpentine, experience significant local amplification (Dave Boore, personal communication). With the exception of these sites, which represent significant contributions to the model variance, the point-source model (Table 1, model 1) with site-specific kappa values provide a good estimate of the observed attenuation of peak acceleration.

EFFECTS OF WAVE PROPAGATION

In both the finite-source and point-source stochostic models presented here, geometrical attenuation was modeled as a simple 1/distance (distance to largest asperity for the point-source) dependency. In order to investigate the effects of accurately accommodating the direct and supercritically reflected rays in the point-source simulations, the method of Ou and Herrmann [2] was employed. This technique computes the appropriate geometrical attenuation and duration for the direct and supercritical rays in a manner appropriate for the stochastic ground motion model.

For a quantative comparison of the response spectral ordinates using the 1/R geometrical attenuation model and the direct plus supercritical model, the standard errors are shown in Figure 8 for both cases using model 1 parameters. The direct plus supercritical shows a larger uncertainty for frequencies greater than about 3 Hz, comparable uncertainty from about 3 Hz to about 0.3 Hz, and then lower levels of uncertainty at long periods. These results indicate that, in the stochastic model, over the period range of several seconds to over 30 Hz, the 1/R geometrical attenuation performs generally as well as the seismologically more rigorous model which includes the direct plus supercritically reflected phases.

CONCLUSIONS

An extension of the stochastic ground motion model which accommodates a finite- source as well as nonlinear soil response has been used to model the source, path, and site effects of the 1989 Loma Prieta earthquake. Based upon an analysis of variance between the observed and computed response spectra, the preliminary results indicate that the finite-fault and point-source models provide comparably low levels of uncertainty. Depending upon oscillator period, both models produce uncertainty levels comparable to the standard errors resulting from empirical regression analyses. Specifically, for sites within about 50 km of the fault, the finite-source provides slightly lower variance estimates while for all distances, the point-source results are generally lower in variance from several seconds to over 30 Hz. Using site-specific kappa values, based upon an inversion of strong motion data recorded at 22 rock sites, the variance is reduced considerably for frequencies above about 3 - 4 Hz.

Comparing the simple 1/R geometrical attenuation assumed for the stochastic model [1] with a seismologically more rigorous model which includes the direct plus supercritically reflected phases [2] resulted in nearly the same estimates of uncertainty. These results indicate that the simple stochastic point-source model with 1/R geometrical attenuation provides a good fit to the response spectra computed from observed records at fault distances varying from 1 - 80 km. For the point-source model, with site specific kappa values, the standard error of peak acceleration estimates at rock sites is about 0.34. Using an average kappa value, the standard error is increased about 40% to about 0.47.

REFERENCES

1. T.C. Hanks and R.K. McGuire, "The Character of High-Frequency Strong Ground Motion, Bulletin of the Seismological Society of America 71: 2071-2095 (1981).

2. G.B. Ou and R. B. Herrmann, "A Statistical Model for Ground Motion Produced by Earthquakes at Local and Regional Distances" Bulletin of the Seismological Society of America 80: 1397-1417 (1990).

3. S.H. Hartzell, "Earthquake Aftershocks as Green's Function", Geophys. Res. Lett.5: 1-4 (1978).

4. J.N. Brune, "Tectonic Stress and the Spectra of Seismic Shear Waves from Earthquakes", J. Geophys. Res. 75: 4997-5009 (1970).

5. J.G. Anderson and S.E. Hough, "A Model for the shape of the Fourier Amplitude Spectrum of Acceleration at High Frequencies", Bulletin of the Seismological Society of America 74:(1984).

6. G.R. Toro, R.K. McGuire and W.J. Silva, "Engineering Model of Earthquake Ground Motion for Eastern North America", EPRI NP-6074, Electric Power Research Institute, 1988.

7. D.J. Wald, D.V. Helmberger, and T.R. Heaton, "Rupture Model of the 1989 Loma Prieta Earthquake from the Inversion of Strong Motion and Broadband Teleseismic Data", submitted to Bulletin of the Seismological Society of America (1990).

8. R.B. Darragh, W.J. Silva, C. Stark, J. Schneider, and J.C. Stepp, "Engineering Characterization of Strong Ground Motion at Rock Sites in North America", Proceedings of the Fourth International Conference on Seismic Zonation, Stanford University, 1991.

9. R.W. Burger, P.G. Somerville, J.S. Barker, R.B. Herrmann, and D.V. Helmberger, "The Effect of Crustal Structure on Strong Ground Motion Attenuation Relations in Eastern North America", Bulletin of the Seismological Society of America. 77: 420-439 (1987).

10. W.B. Joyner and D.M. Boore, "On Simulating Large Earthquakes by Green's Function Addition of Smaller Earthquakes", Proceedings of the Fifth Maurice Ewing Symposium on Earthquake source Mechanics, American Geophysical Union, 1986.

TABLE 1
A) Loma Prieta Modeling Summary.

Site Name	Label	Kappa (sec) Model 0	Kappa (sec) Model 1	Fault Dist (km)	PGA(g) Avg. Obs.	PGA(g) Finite Model 0	PGA(g) Finite Model 1	PGA(g) Point* Model 0	PGA(g) Point* Model 1
Corralitos	COR	0.055	0.074	1	0.55	0.52	0.52	0.58	0.53
Gilroy 1	GL1	0.025	0.043	15	0.44	0.43	0.29	0.51	0.43
Gilroy 2	GL2	0.040	0.052	16	0.35	0.39	0.36	0.41	0.41
UC Santa Cruz	UCS	0.040	0.037	16	0.46	0.51	0.51	0.35	0.44
Gilroy 6	GL6	0.050	0.065	24	0.14	0.17	0.16	0.23	0.23
Palo Alto VA Hosp.	PAV	0.040	0.052	24	0.37	0.38	0.38	0.38	0.34
SLAC	SLA	0.060	0.062	28	0.24	0.19	0.17	0.16	0.19
Redwood City-Cañada	RDC	0.120	0.072	38	0.07	0.09	0.14	0.07	0.13
SAGO South	SAS	0.100	0.082	39	0.07	0.07	0.08	0.08	0.12
APEEL 7	A07	0.100	0.058	44	0.13	0.09	0.14	0.07	0.12
APEEL 10	A10	0.100	0.078	44	0.09	0.09	0.11	0.07	0.10
Monterey City Hall	MON	0.060	0.054	44	0.07	0.11	0.11	0.09	0.12
Belmont 2-story Bldg	BEL	0.080	0.067	46	0.11	0.12	0.13	0.08	0.11
Apeel 2E CUSH Stad.	A2E	0.040	0.059	53	0.08	0.08	0.06	0.09	0.09
Sierra Point	SSP	0.040	0.029	65	0.08	0.10	0.10	0.07	0.09
SF Diamond Heights	SFD	0.040	0.039	73	0.10	0.09	0.08	0.07	0.09
Piedmont Jr. High	PHS	0.050	0.042	74	0.08	0.06	0.07	0.06	0.08
SF Rincon	SFR	0.040	0.018	76	0.09	0.09	0.11	0.07	0.10
Yerba Buena Island	YBI	0.080	0.080	77	0.05	0.06	0.08	0.05	0.06
SF Pacific Heights	SFH	0.080	0.055	78	0.06	0.09	0.07	0.05	0.07
SF Telegraph Hill	SFT	0.040	0.048	78	0.07	0.08	0.07	0.06	0.07
SF Presidio	SFP	0.080	0.033	79	0.16	0.08	0.08	0.05	0.08
Treasure Island	TRI	0.040	0.052	79	0.13	0.14	0.14	0.14	0.14
SF Cliff House	SFC	0.080	0.048	80	0.09	0.05	0.07	0.04	0.07
SF Golden Gate	SFG	0.040	0.036	81	0.18	0.08	0.07	0.06	0.08
		AVG.** 0.06	AVG.** 0.05						

*Point source simulations use a source depth of 12 km (depth of largest asperity [7]).

**Average of rock sites

B) Source Parameters and Path Q Models

Model	M	SD (Bars)	Duration (sec)	Q_0	ETA
0	6.90	238	6.0	150	0.60
1	6.86	184	6.2	186	0.36

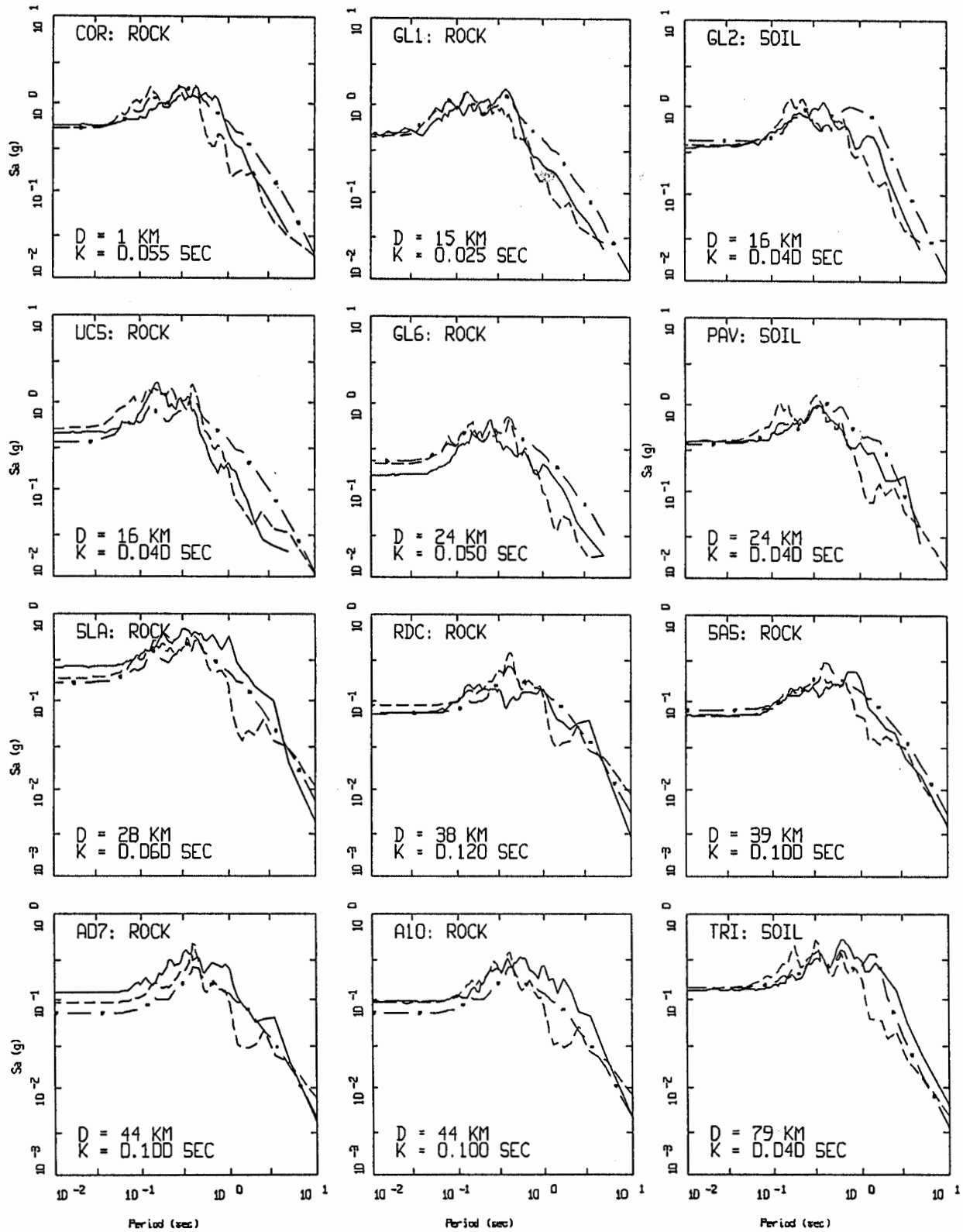

Figure 1. 5% damped response spectra for Loma Prieta earthquake at 9 rock and 3 soil sites in SF Bay Area. Shown for each site are observed data (solid), and simulations from finite fault (dashed) and point source (dash-dotted). Model parameters are shown in Table 1 (model 0).

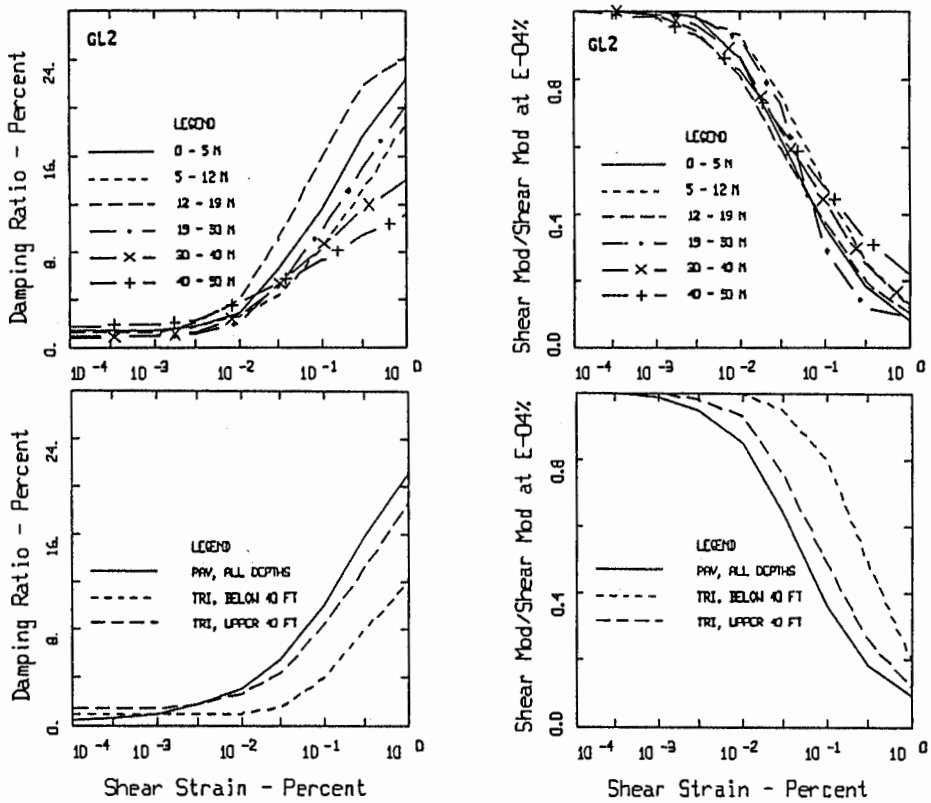

Figure 2. Modulus reduction and damping models for soil sites GL2, PAV, and TRI.

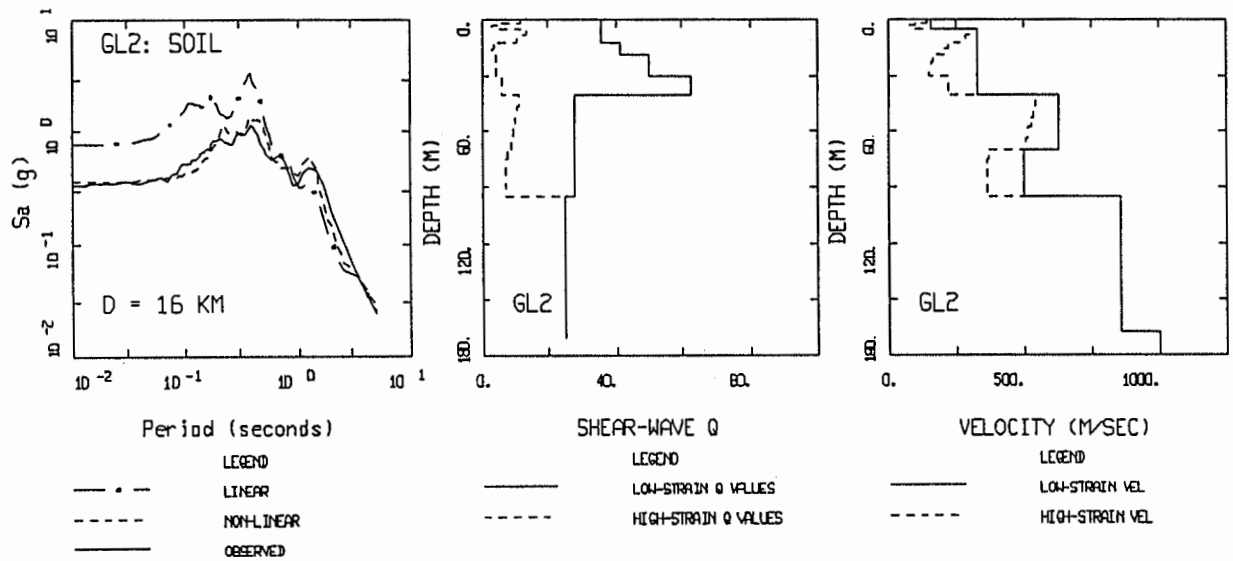

Figure 3. Results of site response analyses at GL2 using linear and equivalent-linear soil response. Rock outcrop motion at GL1 (vector sum Fourier spectra) was used as control motion. Left frame is 5% damped response spectral acceleration showing results of linear and equivalent-linear analyses. Center frame shows the initial (low-strain) and final (high-strain) soil Q profile (damping $\approx$ 1/2Q). Right frame shows the initial and final shear wave velocities. Initial (low-strain) shear wave Q is taken from the laboratory data at 10^{-4}% shear strain.

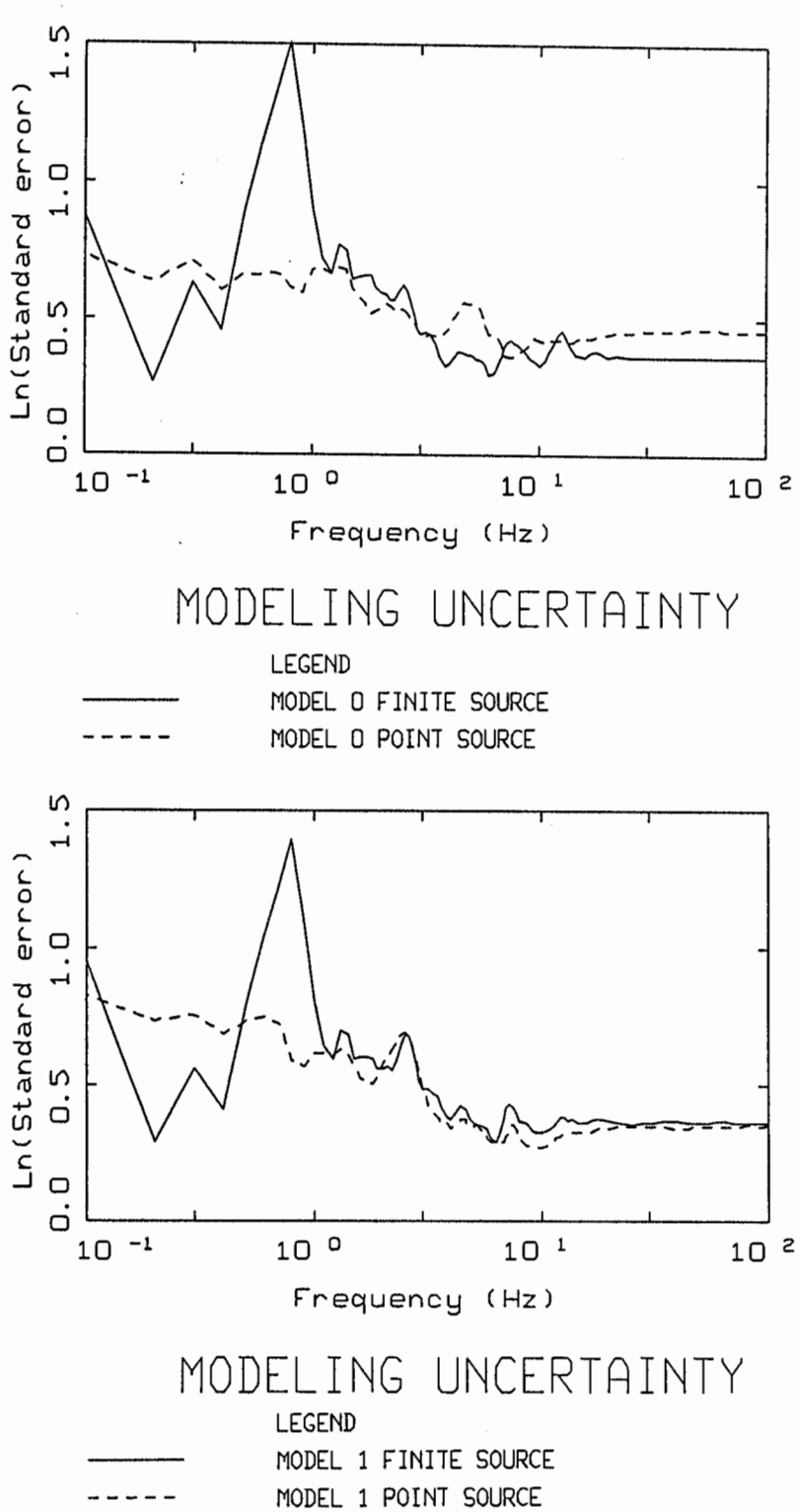

Figure 4. Plot of natural logarithm of the standard error of response spectral ordinates for finite and point source model computation at all rock sites using model 0 (upper) and model 1 (lower). Model parameters are shown in Table 1.

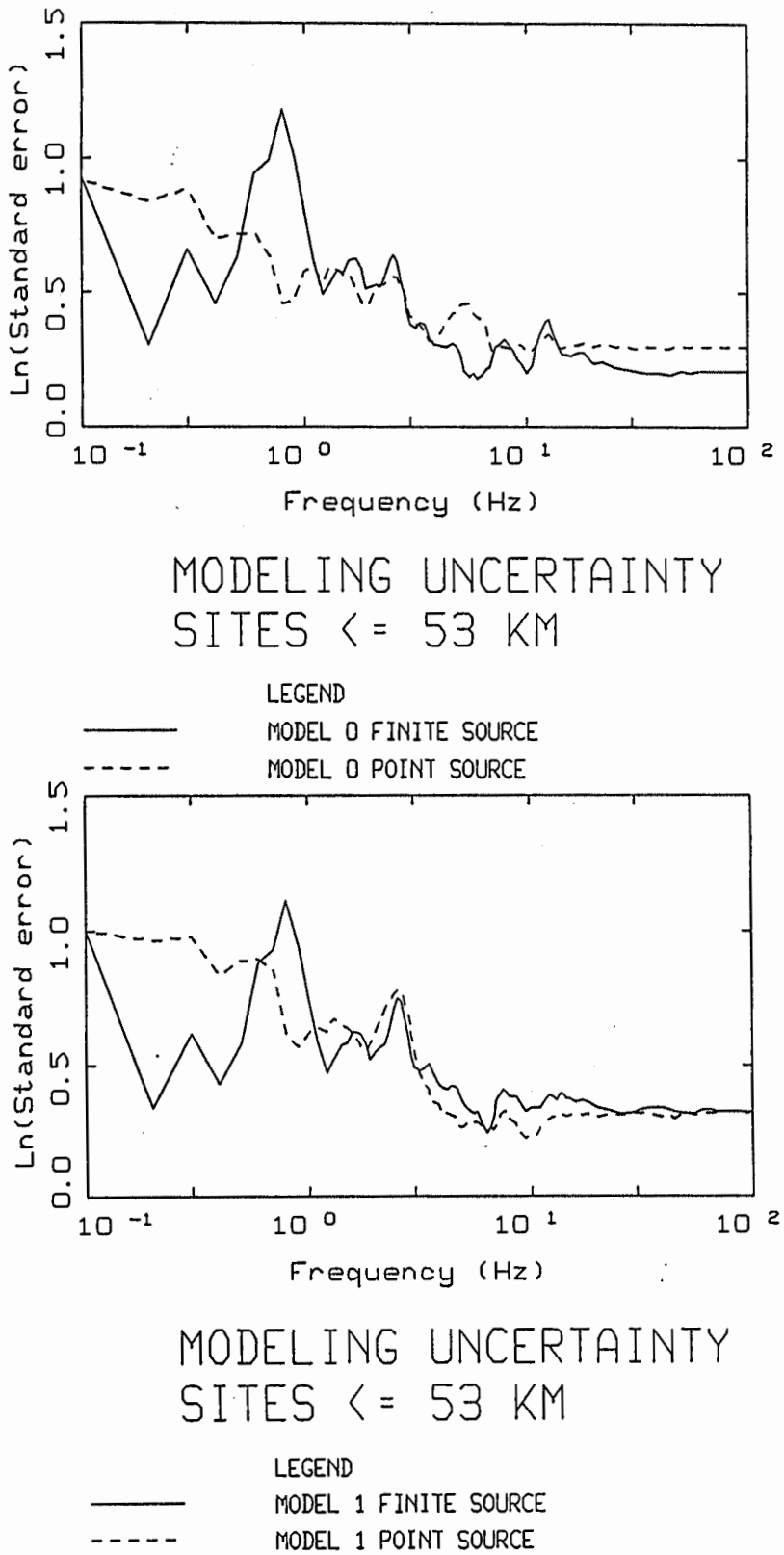

Figure 5. Plot of natural logarithm of the standard error of response spectral ordinates for finite and point source model computation at sites less than 55 km using model 0 (upper) and model 1 (lower). Model parameters are shown in Table 1.

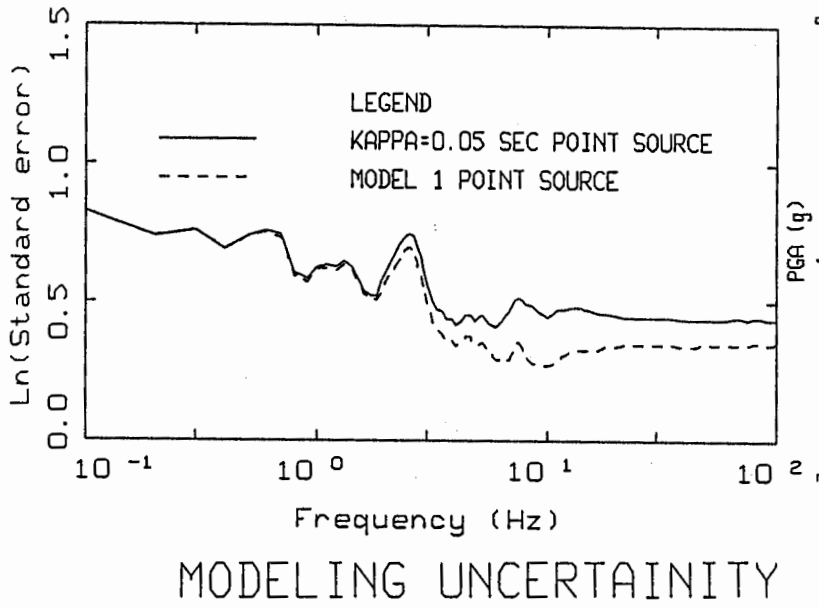

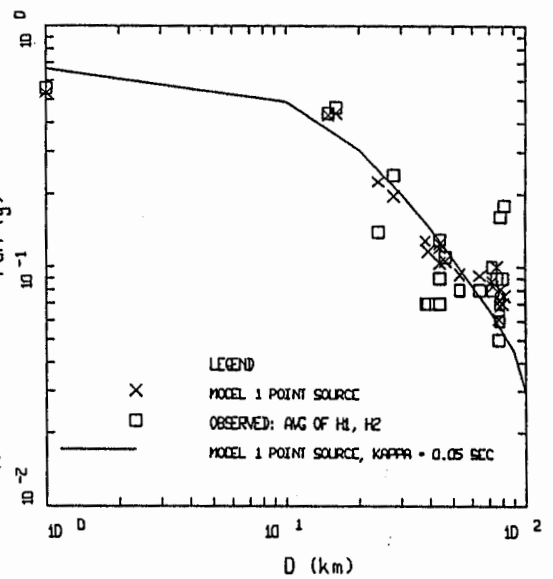

Figure 6. Left. Plot of natural logarithm of the standard error of response spectral ordinates for the point source model computation using model 1. Solid line uses a constant kappa value of 0.05 sec. Model parameters are shown in Table 1.

Figure 7. Right. Plot of peak acceleration attenuation: squares, average of the observed horizontal components; crosses, model 1 using site specific kappa values; solid line, model 1 with average kappa value.

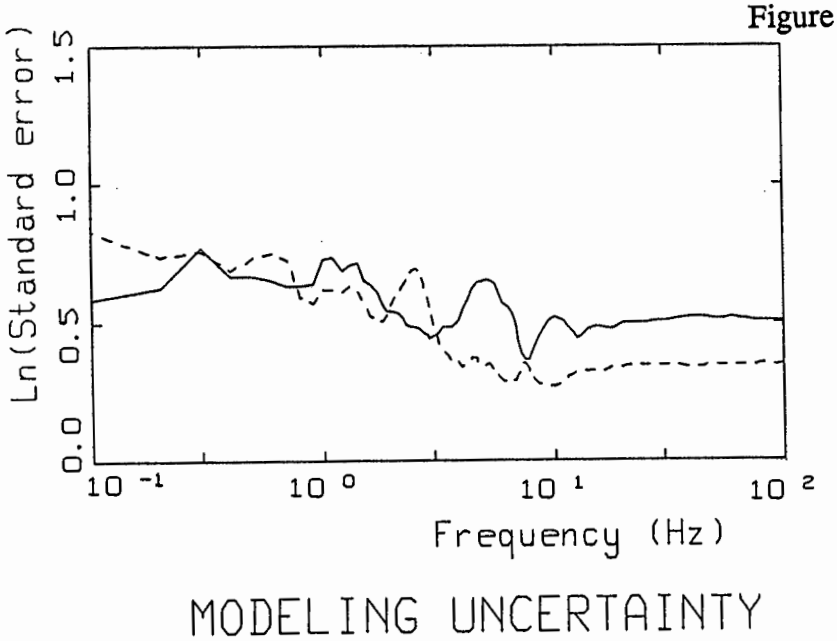

Figure 8. Plot of natural logarithm of the standard error of response spectral ordinates for the point source model computation using model 1. Solid line includes the direct plus supercritically reflected phases. Dashed line is for the simple 1/R geometrical attenuation. Model parameters are shown in Table 1.